# Full-color autostereoscopic 3D display system using color-dispersion-compensated synthetic phase holograms

**Kyongsik Choi, Hwi Kim, and Byoungho Lee**

*National Research Laboratory of Holography Technologies*
*School of Electrical Engineering, Seoul National University, Seoul 151-744, Korea*
*Phone: +82-2-880-7245, Fax: +82-2-873-9953*
*byoungho@snu.ac.kr*

*http://oeqelab.snu.ac.kr*

**Abstract:** A novel full-color autostereoscopic three-dimensional (3D) display system has been developed using color-dispersion-compensated (CDC) synthetic phase holograms (SPHs) on a phase-type spatial light modulator. To design the CDC phase holograms, we used a modified iterative Fourier transform algorithm with scaling constants and phase quantization level constraints. We obtained a high diffraction efficiency (~90.04%), a large signal-to-noise ratio (~9.57dB), and a low reconstruction error (~0.0011) from our simulation results. Each optimized phase hologram was synthesized with each CDC directional hologram for red, green, and blue wavelengths for full-color autostereoscopic 3D display. The CDC SPHs were composed and modulated by only one phase-type spatial light modulator. We have demonstrated experimentally that the designed CDC SPHs are able to generate full-color autostereoscopic 3D images and video frames very well, without any use of glasses.



**OCIS codes:** (070.2580) Fourier optics, (090.0090) Holography, (090.1760) Computer holography, (090.2870) Holographic display, (100.6890) Three-dimensional image processing, (230.6120) Spatial light modulators.

---

## References and Links

1. Y. Kim, J.-H. Park, H. Choi, S. Jung, S.-W. Min, and B. Lee, “Viewing-angle-enhanced integral imaging system using a curved lens array,” Opt. Express **12**, 421-429 (2004), http://www.opticsexpress.org/abstract.cfm?URI=OPEX-12-3-421
2. B. Lee, S.-W. Min, and B. Javidi, “Theoretical analysis for three-dimensional integral imaging systems with double devices,” Appl. Opt. **41**, 4856-4865 (2002).
3. P. S. Hilaire, S. A. Benton, and M. Lucente, “Synthetic aperture holography: a novel approach to three dimensional displays,” J. Opt. Soc. Am. A **9**, 1969-1977 (1992).
4. M. Lucente and T. A. Galyean, “Rendering interactive holographic images,” in *Computer Graphics and Interactive Techniques*, S. G. Mair, eds., Proc. SIGGRAPH **95**, 387-394 (1995).
5. J. H. Kulick, G. P. Nordin, A. Parker, S. T. Kowel, R. G. Lindquist, M. Jones, and P. Nasiatka, “Partial pixels: a three-dimensional diffractive display architecture,” J. Opt. Soc. Am. A **12**, 73-83 (1995).
6. J. Yan, S. T. Kowel, H, J. Cho, and C. H. Ahn, “Real-time full-color three-dimensional display with a micromirror array,” Opt. Lett. **26**, 1075-1077 (2001).
7. K. Choi, H. Kim, and B. Lee, "Synthetic phase holograms for autostereoscopic image displays using a modified IFTA," Opt. Express 12, 2454-2462 (2004), http://www.opticsexpress.org/abstract.cfm?URI=OPEX-12-11-2454
8. H. H. Suh, "Color-image generation by use of binary-phase holograms," Opt. Lett. **24**, 661-663 (1999).
9. U. Levy, E. Marom, and D. Mendlovic, "Simultaneous multicolor image formation with a single diffractive optical element," Opt. Lett. **26**, 1149-1151 (2001).

#5297 - $15.00 US Received 14 September 2004; revised 11 October 2004; accepted 11 October 2004

10. K. Choi, B. Choi, Y. Choi, S. Kim, J. Kim, N. Kim, and S. Gil, "Multiphase computer-generated holograms for full-color image generation," in Practical Holography XVI and Holographic Materials VIII, S. A. Benton, S. H. Stevenson, and T. J. Trout, eds., Proc. SPIE **4659**, 242-249 (2002).
11. S. Fukushima, T. Kurokawa, and M. Ohno, "Real-time hologram construction and reconstruction using a high-resolution spatial light modulator," Appl. Phys. Lett. **58**, 787-789 (1991).
12. J. W. Goodman, *Introduction to Fourier Optics*, 2nd ed., (McGraw-Hill, New York, 1996).
13. A. W. Lohmann and D. P. Paris, "Computer generated spatial filters for coherent optical data processing," Appl. Opt. **7**, 651-655 (1968).
14. G. Tricoles, "Computer generated holograms: an historical review," Appl. Opt. **26**, 4351-4360 (1987).
15. N. Mukohzaka, N. Yoshida, H. Toyoda, Y. Kobayashi, and T. Hara, "Diffraction efficiency analysis of a parallel-alighned nematic-liquid-crystal spatial light modulator," Appl. Opt. **33**, 2804-2811 (1994).
16. U. Efraon, S. T. Wu, and T. D. Bates, "Nematic liquid crystals for spatial light modulators: recent studies," J. Opt. Soc. Am. B **3**, 247-252 (1986).
17. J. Gourlay, S. Samus, P. McOwan, D. G. Vass, I. Underwood, and M. Worboys, "Real-time binary phase holograms on a reflective ferroelectric liquid-crystal spatial light modulator," Appl. Opt. **33**, 8251-8254 (1994).
18. R. W. Gerchberg and W. O. Saxton, "A practical algorithm of the determination of the phase from image and diffraction plane pictures," Optik **35**, 237-246 (1972).
19. F. Wyrowsiki, "Diffractive optical elements: iterative calculation of quantized, blazed phase structures," J. Opt. Soc. Am. **7**, 961-969 (1990).
20. J. R. Fienup, "Phase retrieval algorithms: a comparison," Appl. Opt. **21**, 2758-2769 (1982).
21. V. A. Soifer, V. V. Kotlyar, and L. Doskolovich, *Iterative Methods for Diffractive Optical Elements Computation* (Taylor & Francis Ltd, 1997).
22. L. Ge, M. Duelli, and R. W. Cohn, "Enumeration of illumination and scanning modes from real-time spatial light modulators," Opt. Express **7**, 403-416 (2000), http://www.opticsexpress.org/abstract.cfm?URI=OPEX-7-12-403
23. T. Iwaii and T. Asakura, "Speckle reduction in coherent information processing," Proc. IEEE **84**, 765-781 (1996).
24. T. Ito and K. Okano, "Color electroholography by three colored reference lights simultaneously incident upon one hologram panel," Opt. Express **12**, 4320-4325 (2004). http://www.opticsexpress.org/abstract.cfm?URI=OPEX-12-18-4320
25. Web sites: http://www.stereoscopy.com, http://www.stereopia.com, and http://www.starosta.com.

## 1. Introduction

Real-time full-color autostereoscopic three-dimensional (3D) display systems, such as integral imaging [1,2], holographic stereography [3,4], partial pixel structures [5], and micro mirror array architecture [6] have been developed and are of interest. Holography is the only 3D imaging technique that is capable of providing all the depth cues, and can produce images with virtually unlimited resolution. In particular, a natural full-color 3D display is one of the goals of holographic display systems. However, the size and complexity of holographic fringe patterns for general digital holography often preclude their computation at interactive rates. Therefore, the cost of calculating samples is high if a conventional approach is taken. However, Fourier synthetic phase holograms (SPHs) provide an excellent design possibility, and make the most efficient use of the hologram space-bandwidth product [7]. Color holograms are basically multiplexed holograms that produce multi-color images. They can be recorded with three wavelengths. When reconstructed with the recording wavelengths, the hologram produces overlapping images in three colors producing a multicolor image. While this has been achieved with various degrees of success, full-color holography is still regarded as being very difficult, due to a number of constraints on the lasers, photo material, and hologram types used, the difficulty of achieving color fidelity, and the low light efficiencies involved.

Recently, we proposed and implemented an SPH for an autostereoscopic 3D display system using a modified iterative Fourier transform algorithm (IFTA) [7]. However, this was a monochromatic hologram, because it had difficulty in achieving a full-color image due to the color dispersion characteristics resulting from the wavelength differences of the illumination sources. To minimize the color difference error between the object and the reconstructed three color components, some other methods [8-10] have been introduced, but

#5297 - $15.00 US Received 14 September 2004; revised 11 October 2004; accepted 11 October 2004

these have had difficulty in reproducing dynamic holograms. The development of spatial light modulators (SLMs) with a high resolution and a fast response time is helping to create dynamic holograms [11]. Dynamic holograms may be used in areas such as beam shaping, optical interconnects, holographic animations, 3D displays, and optical computing [12-14].

In this paper, for the first time to our knowledge, we propose and implement a dynamic autostereoscopic 3D display system using color-dispersion-compensated (CDC) SPHs implemented with only one phase-type SLM. This can be integrated easily using only an SLM, three laser sources, and a projection lens module, and also it has advantages in cost-effectiveness, a high light source utilization efficiency, and controllable color fidelity without the use of any color filters.

## 2. Principle of the proposed full-color video display system

We will now discuss the operating principle of the full-color autostereoscopic 3D display system and the method of making the CDC SPHs. Figure 1 shows a schematic diagram of our proposed full-color autostereoscopic 3D display system.

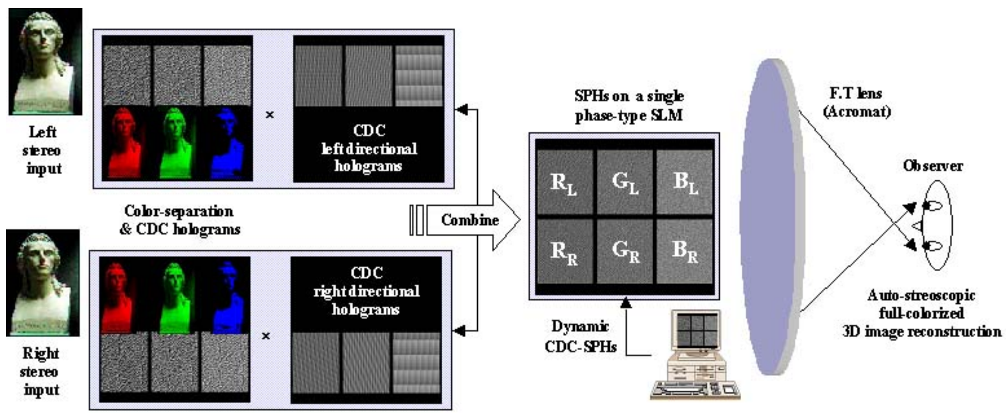


Fig. 1. Schematic diagram of our proposed full-color autostereoscopic 3D display system

In Fig. 1, each left or right stereo input image is separated into three primary color components; i.e., red, green, and blue images. Each target image is encoded using two-dimensional phase-only information using our modified IFTA. The modified IFTA has scaling constraints for color dispersion compensation and different phase quantization levels for compensating the phase difference error with respect to each red, green, and blue light source. The encoded CDC holograms are then synthesized using each directional hologram for supplying the direct viewing conditions to an observer without the use of any glasses. Each synthesized CDC phase hologram is combined using a phase-type SLM. The phase-modulated information is converted to a simple Fourier transform using an achromatic lens for an autostereoscopic 3D display to an observer without color dispersion. Due to the symmetry of the lens, the synthesized phase holograms are placed in a symmetrical position about the center axis of the lens in the SLM plane. In addition, special attention must be paid to satisfying the stereo viewing conditions, such as the viewing distance, the viewer's eye separation, and the viewer's eye pupil size, to achieve a 3D stereo depth effect. In our work, we assumed that the stereo viewing conditions were as follows: the observer's viewing distance, eye separation, and pupil size were 300, 65, and 3 mm, respectively. To reconstruct the full-color autostereoscopic 3D display we used three illumination sources with wavelengths of $\lambda$ = 635 nm (red), 532 nm (green), and 473 nm (blue). The size of the designed CDC SPHs was 256×256. The minimum pixel size of the phase-type SLM was about 32 μm. The achromatic Fourier transform lens had a focal length of 300 mm.

From scalar diffraction theory [12], the light complex amplitude in the hologram plane (the SLM plane), $W(\xi,\eta) = A(\xi,\eta)\exp[i\phi(\xi,\eta)]$, is related to the light complex amplitude in the observation plane, $\hat{F}(x,y) = \hat{A}(x,y)\exp[i\hat{\phi}(x,y)]$ (The intensity distribution, $I(x,y)$, is the absolute square of the complex amplitude distribution) via the following Fresnel integral transform:

$$\hat{F}(x,y) = \frac{1}{j\lambda z}\exp\left(j\frac{2\pi z}{\lambda}\right)\int_{-\infty}^{\infty}\int W(\xi,\eta)H(x-\xi,y-\eta)d\xi d\eta, \tag{1}$$

where $z$ is the propagation distance, $H(u,v) = \exp\left[j\pi/(\lambda z)\left(u^2+v^2\right)\right]$ is the transfer function of propagation through free space, and $\lambda$ is the wavelength of the reconstructing illumination light. For a Fourier transform using a lens of focal length $f$, it is known that Eq. (1) can be reformed as a Fourier transform from $(\xi,\eta)$ space to $(x/(\lambda f), y/(\lambda f))$ space [12]. Hence the reconstructed image size is proportional to the light wavelength, as $x$ increases with $\lambda$ for a constant value of $x/(\lambda f)$. Each calculated size of the reconstructed color image components in the image plane was about 6, 5, and 4.4 mm, respectively, without scaling. Because we used three laser sources with wavelengths of $\lambda$ = 635 (red), 532 (green), and 473 nm (blue), respectively, these reconstructed and superposed stereo color images should be inversely scaled with respect to these image sizes to minimize the color difference error in the modified IFTA optimization process. We obtained the scale ratio of 1/635:1/532:1/473 ≅ 0.7449:0.8378:1 for red, green, and blue target component images. In addition, these had to be magnified by a projection lens module to satisfy the predefined autostereoscopic viewing conditions.

First, we separated a full-color image into three target images corresponding to the red, green, and blue components, and adjusted the size of each target image to the precalculated scale ratio. Then, we used the modified IFTA with different phase quantization levels for applying each hologram to a single-phase-type SLM. To satisfy the direct 3D viewing condition, we synthesized CDC phase holograms with corresponding left and right directional holograms. The directional holograms were compensated for color dispersion, as the diffraction angle is dependent on the wavelength for the same directional hologram. For example, we can determine how much each color is deviated using the grating equation, $d\sin\theta = m\lambda$. As we used a minimum pixel size 32 μm for the SLM, we could calculate each diffraction angle, $\theta_R = 1.137^\circ$, $\theta_G = 0.9526^\circ$, and $\theta_B = 0.8469^\circ$, respectively. Therefore, these diffraction angles were also compensated for in our modified IFTA process. Finally, we placed all the designed phase holograms on one SLM to obtain a dynamic full-color holographic display.

To dynamically control the CDC SPHs using only one phase-type SLM, we applied a phase quantization leveling as a phase-compensation method in our modified IFTA optimization process. Some SLMs, such as parallel-aligned nematic liquid crystals (NLCs) [15], twisted nematic liquid crystals (TNLCs) [16], and ferroelectric liquid crystal structures [17], can work as phase-only or amplitude modulators, depending on the applied voltage. In general, the voltage control of an SLM can be supplied by the gray-level signals ranging from 0 ~ 255. The phase retardation for an NLC is given by:

$$\Delta\phi = \begin{cases} \alpha\phi_m(V/V_0 - 1), & if\ (V-V_0)/V_0 << 1 \\ \phi_m(1-\beta/V), & if\ (V-V_0)/V_0 >> 1 \end{cases} \tag{2}$$

where $\phi_m (= 2\pi d\Delta n/\lambda)$ is the maximum phase shift, $d$ is the thickness of the liquid crystal layer, $\Delta n$ is the difference of the refraction indexes of the liquid crystal depending on the polarization, $V_0$ is the threshold voltage, and $\alpha$ and $\beta$ are known functions of the elastic constants and the dielectric anisotropy of the liquid crystal, respectively. To reduce the phase difference error, $\Delta\phi_m^i$, the maximum phase shift, $\phi_m$, should have the same value of 2π for all phase holograms. However, in fact it is dependent on the illumination wavelength as follows:

$$\Delta\phi_m^i = 2\pi d\Delta n\left(\frac{1}{\lambda_0}-\frac{1}{\lambda_i}\right),\ (i = R, G, B) \tag{3}$$

where $\lambda_0$ is the originally intended wavelength of the SLM, and $\lambda_i$ is the reconstruction wavelength for full-color hologram. In our case, we used three laser diodes with the wavelengths of $\lambda_0$ = 532 nm ($\lambda_G$, green), 635 nm ($\lambda_R$, red), and 473 nm ($\lambda_B$, blue). The maximum phase modulation of 2π was achieved in our SLM for green light with a wavelength of 532 nm. Thus, we could obtain the maximum phase shift, $\phi_m^R = 0.84\times(2\pi)$, $\phi_m^G = (2\pi)$, and $\phi_m^B = 1.12\times(2\pi)$ with respect to the reconstruction wavelengths of the red, green, and blue light sources. This phase quantization leveling is applied as a phase constraint in our modified IFTA to optimize each red, green, and blue target image without any phase difference error. In general, the voltage control of the SLM can be supplied by the gray-level signals ranging from 0 to 255. Therefore, the maximum phase shift under green light was matched to the gray-level signal value of 255. The 0-255 gray-scale signal gave a 0-2π phase modulation for the green light source, but gave a 0-1.68π and 0-2.24π phase modulation for the red and blue light sources, respectively. The applied gray-scale signals for red, green and blue were adjusted with proper scaling to induce the different quantized phase levels for each color.

## 3. Modified IFTA and simulation results

IFTA is an efficient and stable numerical design method, and many practical variants of the IFTA method have been proposed and investigated [18-21]. All these methods consist of two stages: one stage involving the Fourier transform, and another stage where the constraints are imposed in both the hologram plane and the image plane. These two stages are repeated until the error between the intensity distribution of the reconstructed image and the target image reaches a predetermined tolerance, or when a predefined number of iterations have been achieved; i.e., this procedure is iterated until the error criterion is satisfied. To design CDC SPHs, the modified IFTA should be considered carefully for imposing constraints, such as the different reconstruction wavelengths, scaling ratio, each phase quantization level, the minimum pixel size of the phase-type SLM, the viewing distance, and the observer's eye separation. Hence, we applied a previously proposed modified IFTA method that could be used to reproduce stereoscopic gray-level intensity images [7]. The error criterion function was defined by Eq. (4) to obtain a high diffraction efficiency, a large signal-to-noise ratio, and a low reconstruction error distribution between the reconstructed gray-level image and the target reconstruction image:

$$\begin{aligned}\varepsilon_0 = {} & \sigma_F \int_{-\infty}^{\infty}\!\!\int \left[\left|\hat{F}(x,y)\right| - B_0(x,y)\right]^2 dxdy + \sigma_S \iint_S \left[\left|\hat{F}(x,y)\right| - B_0(x,y)\right]^2 dxdy \\ & + \sigma_N \iint_N \left|\hat{F}(x,y)\right|^2 dxdy + \alpha_D \iint_S \left[\left(\partial_x\left|\hat{F}\right|\right)^2 + \left(\partial_y\left|\hat{F}\right|\right)^2\right] dxdy\end{aligned} \tag{4}$$

where, $B_0(x,y) = \sqrt{\left|I_0(x,y)\right|}$, $I_0(x,y)$ is quantized by a predefined gray-level value of $2^5$, $\sigma_F$, $\sigma_S$, and $\sigma_N$ are the relaxation parameters, and $\alpha_D$ is the regularization parameter for smoothness control without reducing the diffraction efficiency of the reconstructed image. We used $\sigma_F$ = 0.5, $\sigma_S$ = 0.5, $\sigma_N$ = 1, and $\alpha_D$ = 0.15, and the subscripts $S$ and $N$ denote the signal region and noise region, respectively. The diffraction efficiency, $I_{DE} = 100\%\times\sum_S I_S / \left(\sum_S I_S + \sum_N I_N\right)$, was defined as the ratio of the diffracted signal beams in the signal region to all the diffracted light that included the light in the noise region. A root mean square error (RMSE) $RMSE = \left[\sum_S (I_S - I_0)^2 / M^2\right]^{1/2}$, which determined the reconstructed image quality, was computed from the difference between the normalized reconstructed image and the normalized target image that contained $M \times M$ pixels. The signal-to-noise ratio was defined as $SNR = 10 \times \log_{10}(I_S / I_N)$. Using our method, we could theoretically obtain a high diffraction efficiency (~90.04%), a large signal-to-noise ratio (~9.57dB), and a low reconstruction error (~0.0011).

To implement the proposed full-color autostereoscopic 3D display system using CDC SPHs, we used two crossed-view stereo color images [25], each with quantized gray-level values of $2^5$, as shown in Figs. 2(a) and 2(b). The sizes of the desired images of a sculpture of Shiller and a kissing scene were 85×126 and 75×108, respectively. Each size of the designed CDC SPHs was 256×256, and the size of the composed hologram was 624×832, which was the same size as the SLM used in our experimental setup. In Figs. 2(c) and 2(d), the different gray levels represented the different phase levels ranging from 0 (black) to 1.68π (white), 0 to 2π, and 0 to 2.24π, respectively. Figures 2(e) and 2(f) show stereo images (simulation) reconstructed from the designed CDC SPHs. The stereo effect of reconstructed stereo images can be observed from these images. However, in our projection system, eye crossing was not required, because the reconstructed images for the left and right eyes are immediately redirected to each of the observer's eyes.

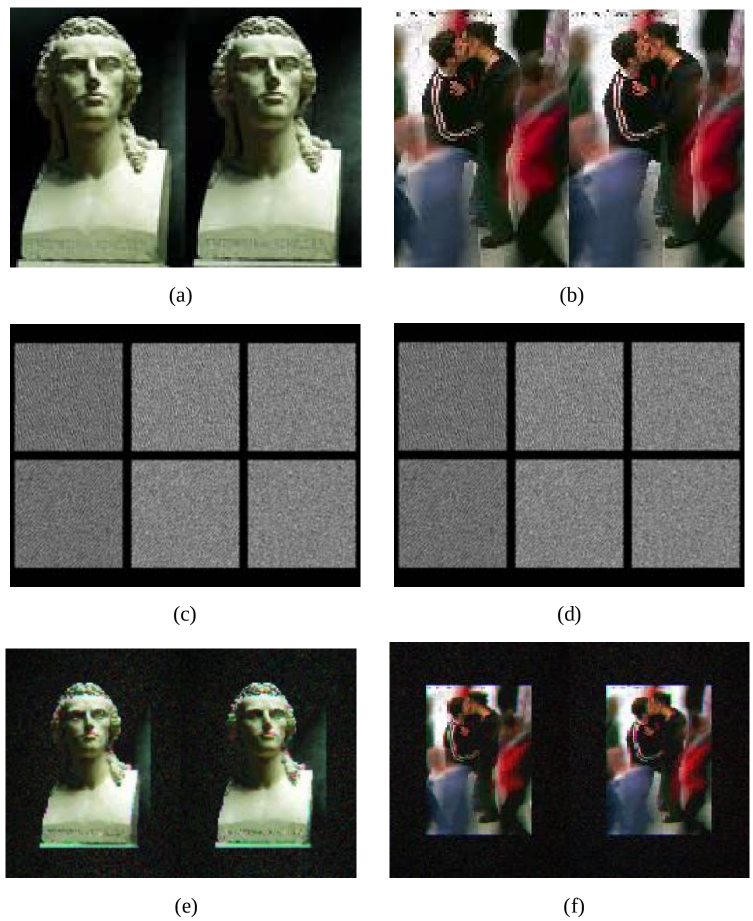


Fig. 2. Stereo input images for: (a) a sculpture of Shiller, and (b) a kissing scene. Images (c) and (d) are the designed CDC SPHs corresponding to (a) and (b), respectively. Images (e) and (f) are the corresponding reconstructed stereoscopic images (simulation).

## 4. Experimental results and discussion

For the experimental verification of our proposed autostereoscopic 3D image and dynamic video display incorporating the designed CDC SPHs, we used a Fourier optic system employing one phase-type SLM, three laser diode sources, and a projection lens module. The optical setup is shown in Fig. 3(a).

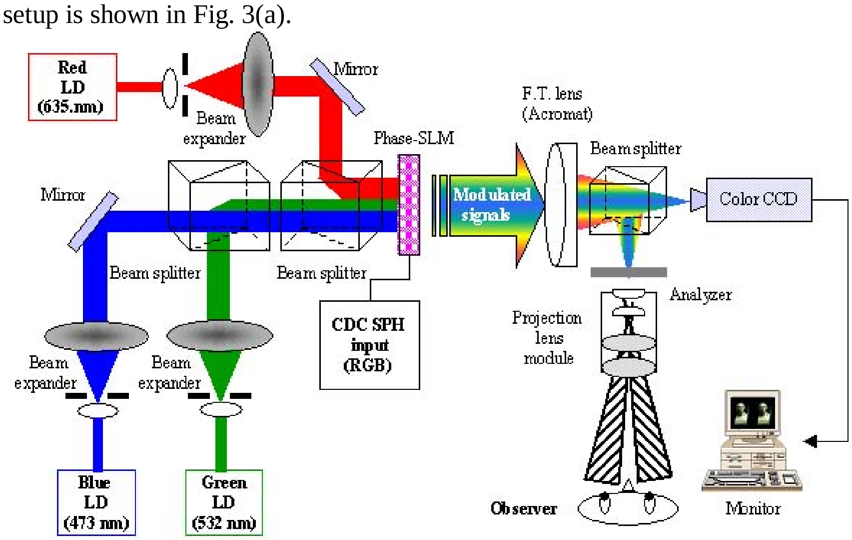


(a)

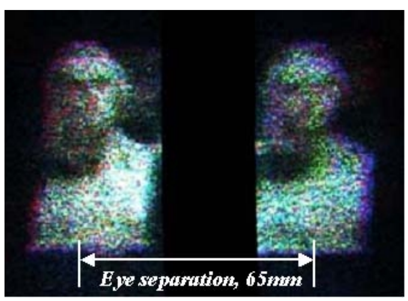


(b)

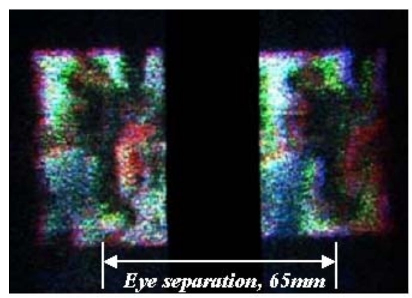


(c)

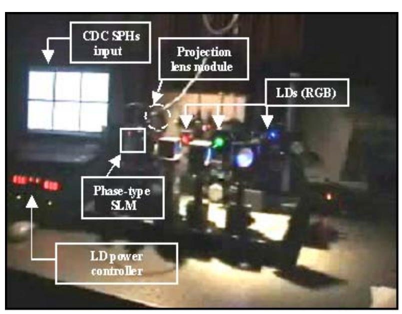


(d)

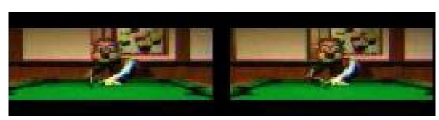

(e)

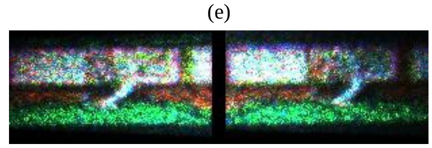

(f)

Fig. 3. (a) Experimental setup of our proposed autostereoscopic display system. (b) Reconstructed image. (c) Images of a sculpture of Shiller and a kissing scene, respectively. (d) Video image of the autostereoscopic 3D demo system. (e) Results of simulation video image, and (f) experimental video image.

First, three laser diode sources with wavelengths of $\lambda$ = 635 nm (red), 532 nm (green), and 473 nm (blue), were collimated and used to illuminate different areas of the SLM. Each laser was modulated by the designed CDC SPHs through the transmissive phase-type SLM (LC-2002, Holoeye). The diffracted beams from the SLM produced an overlapped full-color stereo image on a color charge coupled device (CCD) plane through a precision achromatic doublet lens (PAC086, Newport) having a focal length of 300 mm. The color CCD (DT1100, MegaPlus) produced photographs of the stereo images using image capturing software (IMAQ, NI).

From the experimental results, shown in Figs. 3(b) and 3(c), each stereoscopic full-color image was well superposed on the CCD plane. The zero-order beam on the optical axis resulted from both the nondiffracted beam and the phase mismatch, because of the nonlinear phase modulation transfer characteristics of the SLM, were blocked by a black mask [22]. Figure 3(d) shows our implemented real-time autostereoscopic 3D display demonstration system. This was integrated on an optical table having an area of 60 $cm^2$. For dynamic display, we constructed a video image with a speed of 5 frames per second using the designed CDC SPHs. Figures 3(e) and 3(f) show the reconstructed video images of the simulation and the experimental results, respectively. We also used a projection lens module (EMP-811, Epson) to produce a real autostereoscopic 3D image and dynamic display in the observer plane without using any glasses, as shown in Fig. 3(a). As a result, we were able to observe a real 3D image with a high depth effect; some speckle problems occurred because we used high coherence laser diodes as the illumination sources. To reduce the speckle noise effect other methods have employed a rotating or vibrating transmission-type diffuser [23] or a partially coherent light source array [24], and these may be usefully applied in our system. The discrepancies between the simulated images and the experimental images are caused by the low transmission efficiency (~30%) of the phase-type SLM used in our system. If an SLM with a high transmission efficiency and a high resolution with a small pixel pitch of the same order as that of visible light (~1 μm) were available, then we would expect to obtain a high-quality 3D display image, as in the ideal simulation results. In addition, a small color dispersion error occurs that is the result of the center-axis mismatch of the designed CDC SPHs on the SLM. This error can be reduced by placing each CDC SPH in circular symmetrical positions on the SLM. In general, the color sensitivity depends on the spectral response of the image-capturing device. To represent a natural full-color autostereoscopic 3D image, we need to control the power ratio of the three illumination sources. In our system, we adjusted the power of each laser diode source to 0.141 μW (red), 0.246 μW (green), and 0.729 μW (blue), respectively, to obtain white color mixing.

## 5. Conclusions

We have proposed and implemented a full-color autostereoscopic 3D display system using CDC SPHs on one phase-type SLM. To reduce the color dispersion and the phase difference error arising from the use of three different laser sources for color superposition, we applied scaling constraints and phase quantization leveling in the modified IFTA optimization process. Using this method, we obtained a high diffraction efficiency (~90.04%), a large signal-to-noise ratio (~9.57dB), and a low RMSE error (~0.0011) in simulated reconstructed images. Each optimized phase hologram was synthesized using each CDC directional hologram for the red, green, and blue wavelengths to achieve a full-color autostereoscopic 3D display. The CDC SPHs were composed and modulated using only one phase-SLM. Experimentally, we demonstrated that the designed CDC SPHs were able to generate full-color autostereoscopic 3D images and video frames very well, without using any glasses. However, some discrepancies between the simulated results and the experimental results occurred due to the low transmission efficiency of our phase-type SLM, some speckle problems, and a little chromatic error.

## Acknowledgments

The authors acknowledge the support by the Ministry of Science and Technology of Korea through the National Research Laboratory Program.

#5297 - $15.00 US　　Received 14 September 2004; revised 11 October 2004; accepted 11 October 2004